

CLIC DAMPING RING OPTICS DESIGN STUDIES

M. Korostelev, F. Zimmermann
 CERN, Geneva, Switzerland

Abstract

In this paper the nonlinearities induced by the short period NbFeB permanent wiggler optimized for the CLIC damping ring and their influence to the beam dynamics are studied.

INTRODUCTION

The required beam parameters for the CLIC main linac were re-optimized in 2004-2005 years. The bunch population was reduced to 2.56×10^9 from 4.2×10^9 . However, the bunch spacing was also reduced to 8 cm from 20 cm in order to provide the design luminosity at the interaction point. The new beam parameters for the CLIC are summarized in the Table 1. The changes of the beam parameters for the linac do not entail significant modification in the damping ring optics. The layout of the damping ring remains the same: two long FODO cell straight sections accommodating 76 wigglers, two TME cell arcs, and four dispersion suppressors connecting the arcs and the straights, forming a racetrack shape.

Taking into account intra-beam scattering that is a strong effect for the CLIC damping ring, the parameters for the damping ring RF cavity have been optimized to yield smaller transverse emittances (see Table. 1). As one can see from the Fig. 1, highest RF voltage and RF frequency at fixed betatron coupling of 0.6 % increase the transverse emittances. Doubling the RF frequency increases both transverse emittances by about 15 %. At the same time the longitudinal emittance decreases by about 30 % (not shown). Moreover, the beam loading at the bunch spacing of 8 cm can be critical. For this reason, the bunch spacing of 16 cm was chosen for the damping ring. The beam extraction scenario for the damping ring was revised. Now it is assumed that two trains are extracted simultaneously and combined using a subsequent delay line and RF deflectors. The advantage is a two times larger bunch spacing in the ring compared with the linac, which alleviates the impact of electron cloud and fast ion instabilities.

FITTING THE WIGGLER FIELD

An analytic magnetic field expansion is commonly used to generate a dynamical map for analyzing the particle dynamics through a damping wiggler. The analytic series of the field, fitted to the numerical field map, must be consistent with Maxwells equations.

Assuming, a periodic field in each co-ordinate plane, the magnetic field model in Cartesian expansion can be ex-

Table 1: CLIC damping ring parameters.

Parameter	Symbol	Value
Nominal e^+ ring energy	γmc^2	2.424 GeV
Ring circumference	C	360 m
No. of bunch trains stored	N_t	14
No. of bunches per one train	N_b	110
Bunch population	P_b	2.56×10^9
Extracted hor. emittance	$\gamma \varepsilon_x$	550 nm
Extracted vert. emittance	$\gamma \varepsilon_y$	3.3 nm
Extracted energy spread	σ_δ	1.26×10^{-3}
Extracted bunch length	σ_s	1.55 mm
Horiz. emittance w/o IBS	$\gamma \varepsilon_{nx0}$	134 nm
Betatron coupling	$\varepsilon_y / \varepsilon_x$	0.6%
X-betatron tune	Q_x	69.82
Y-betatron tune	Q_y	34.86
Synchrotron tune	Q_s	0.005
Damping time	$\tau_{x/y}$	2.81 msec
Damping time	τ_s	1.405 msec
Energy loss per turn	U_0	2.074 MeV
Momentum compaction	α_p	0.8×10^{-4}
RF voltage	V_m	2.4 MV
RF frequency	f_{rf}	1875 MHz
Harmonic number	h	2250
Revolution time	T_{rev}	1.213 μs
Repetition rate	f_{rep}	150 Hz
Wiggler parameters		
Number of the wigglers	N_w	76
Wiggler period	λ_w	10 cm
Magnet gap	g	12 mm
Pole width	L_p	60 mm
Field amplitude	B_w	1.7 T
Wiggler length	L_w	2 m

pressed by [1]

$$B_y = \sum_{m,n} c_{mn} \cos(mk_x x) \cos(nk_z z) \cosh(k_{y,mn} y)$$

By using 2D Fourier transform, the coefficients c_{mn} can be derived from the field data. The main disadvantage of the Cartesian expansion is that a large number of modes are needed to achieve good agreement between the fitted field and the real field map. Also the requirement of periodicity in x is not the general case.

The cylindrical expansion of the magnetic field matches natural periodicity in azimuthal coordinate. Multipole expansion [2] of magnetic field in cylindrical and Cartesian coordinates can be expressed by the so-called generalized

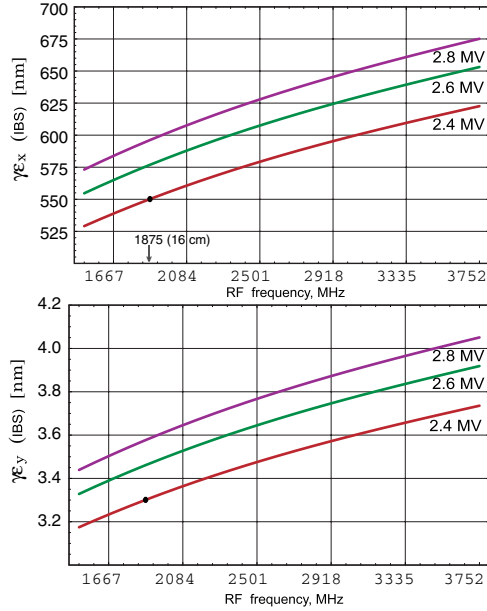


Figure 1: Horizontal and vertical normalized emittance as a function of RF frequency at the three different rf voltages which are 2.8, 2.6 and 2.4 MV.

gradients $C_m(z)$ and their derivatives $C_m^{[k]}$. It should be noted, that $C_m^{[2k+2]} = \frac{d^2}{dz^2} C_m^{[2k]}$. M. Venturini's paper [2] describes the field data representation by using generalized gradients in details.

It is easy to calculate the generalized gradients from numerical field data, if the radial component $B_\rho(\rho = R, \phi, z)$ of the magnetic field is known on a cylindrical surface with radius R . Then the generalized gradients can be found as

$$C_m^{[k]} = \frac{1}{\lambda_w 2^m m!} \sum_{p=-\infty}^{\infty} i^k \frac{(2\pi p / \lambda_w)^{m+k-1}}{I_m'(2\pi p R / \lambda_w)} e^{i 2\pi p z / \lambda_w} \times \int_0^{\lambda_w} e^{-i 2\pi p z / \lambda_w} B_m(R, z) dz \quad (1)$$

where

$$B_m(R, z) = \frac{1}{\pi} \int_0^{2\pi} \sin(m\phi) B_\rho(R, \phi, z) d\phi \quad (2)$$

The modified Bessel functions $I_m(x)$ grow exponentially for large arguments which damps the high frequency harmonics of the magnetic field data.

A tentative design of the NdFeB permanent wiggler [3] which is based on the wiggler design developed by BINP for the PETRA-3 ring, is considered for the CLIC damping ring as a possible variant. The parameters of the PETRA-3 wiggler (wiggler period, gap, field amplitude) were re-optimized to meet CLIC damping ring requirements. Design parameters of the NdFeB wiggler for the CLIC damping ring are summarized in Table 1.

The cylindrical expansion of a magnetic field was fitted to the numerical field map generated by Mermaid code for

one period of this wiggler. Using the largest radius $R = 5 \text{ mm}$, the radial component $B_\rho(R, \phi, z)$ of the magnetic field on the cylinder surface was computed. Taking Fourier integral (2) for the $m = 9$ mode numbers, the profiles of the generalized gradient $C1(z)$, $C3(z)$, $C5(z)$ and their derivatives were found as shown in Fig. 2. It is easy to convert

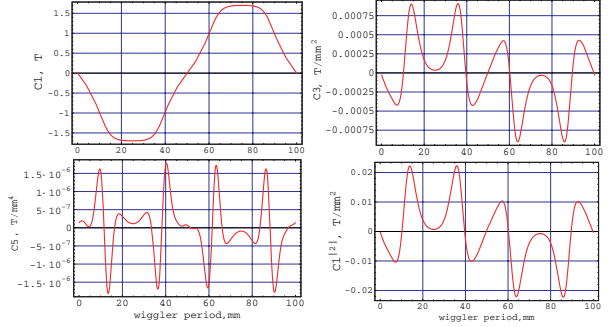


Figure 2: The Generalized gradient $C1(z)$, $C3(z)$ 3^{rd} (sextupole), $C5(z)$ 5^{th} (decapole) order and the second derivative of $C1(z)$.

the cylindrical field representation to the Cartesian form by the following relations: $B_x = B_\rho \cos \phi - B_\phi \sin \phi$, $B_y = B_\rho \sin \phi + B_\phi \cos \phi$. For example, the expression for the vertical field components through 4^{th} can be written as:

$$B_y = C_1 - \left(\frac{C_1^{[2]}}{8} - 3C_3 \right) x^2 - \left(\frac{3C_1^{[2]}}{8} + 3C_3 \right) y^2 + \left(\frac{C_1^{[4]}}{192} - \frac{3C_3^{[2]}}{16} + 5C_5 \right) x^4 + \left(\frac{C_1^{[4]}}{32} - \frac{3C_3^{[2]}}{8} - 30C_5 \right) x^2 y^2 + \left(\frac{5C_1^{[4]}}{192} - \frac{5C_3^{[2]}}{16} + 5C_5 \right) y^4 \quad (3)$$

The close correspondence between the analytical field and the numerical field data is shown in Fig. 3. The blue points represent the numerical field data from Mermaid code, while the red curves show the results of the analytical fit Eq. (3) based on the generalized gradients. At the expected range of validity ($Y = 5 \text{ mm}$ and $X = 60 \text{ mm}$) the field map is in good agreement with the analytical fit.

A transverse kick produced by the one 10 cm wiggler period can be evaluated analytically.

$$x'' = \frac{-e}{p\sqrt{1+x'^2+y'^2}} \left[y' B_s - (1+x'^2) B_y + x' y' B_x \right]$$

$$y'' = \frac{e}{p\sqrt{1+x'^2+y'^2}} \left[x' B_s - (1+y'^2) B_x + x' y' B_y \right]$$

Determining the particle dynamics, one could assume that the horizontal X and vertical Y particle displacements with respect to the reference orbit X_0 remain the constant through one wiggler period. In this case the transverse

DYNAMIC APERTURE

The dynamic aperture of the damping ring in the presence of the wiggler nonlinearities was computed by the BETA code [4]. In the BETA code, an insertion device, for example a wiggler magnet, is described by two interpolation tables, which provide the transverse kicks in both planes as a function of the actual coordinates. Such tables as an input data file for the BETA code were computed by using Eq.(1),(2), (3) and (4). Then, the dynamic aperture of the damping ring for the nonlinear wiggler field model was simulated by BETA as could be seen in Fig. 5 (in terms of sigma for the injected beam). The influence of the nonlinear wiggler field on the dynamic aperture has a weak effect compared to the effect that is produced by the strong sextupoles needed for the chromatic correction. The lattice of the CLIC damping ring requires a small value of the optical functions to achieve ultra low emittances which are $\gamma\epsilon_x = 550$ nm and $\gamma\epsilon_y = 3.3$ nm. The small beta and dispersion functions require a sufficient number of strong sextupoles in order to correct the large horizontal and vertical chromaticities. The sextupoles are arranged by the second-order achromat when two sextupoles with equal strength are separated by a $-I$ transformer. However, the sextupoles introduce significant nonlinearities which limit the dynamic aperture.

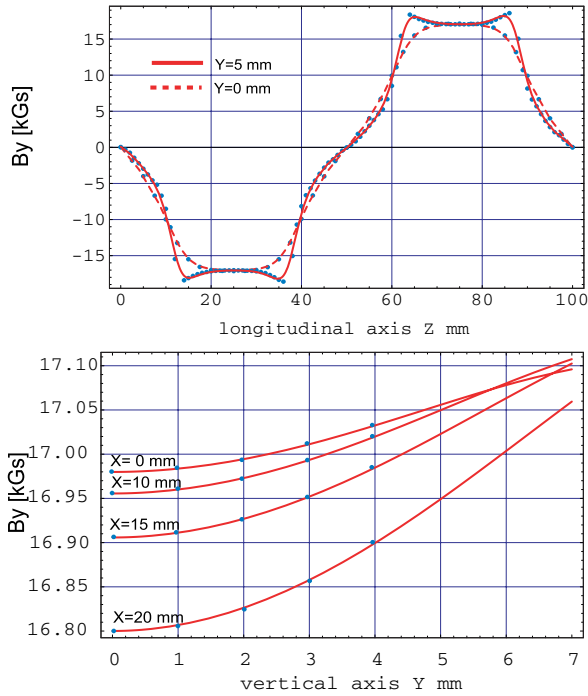


Figure 3: The correspondence between numerical field data and the analytical fit based on the generalized gradients.

kicks produced by the field in one wiggler period can be simplified as

$$\Delta p_x = \frac{e}{p} \int_0^{\lambda_w} B_y(X_0(z) + X, Y, z) dz$$

$$\Delta p_y = \frac{e}{p} \int_0^{\lambda_w} (B_x(X_0(z) + X, Y, z) - \frac{dX_0(z)}{dz} B_z(X_0(z) + X, Y, z)) dz \quad (4)$$

The reference orbit amplitude in the wiggler is $55 \mu m$. The

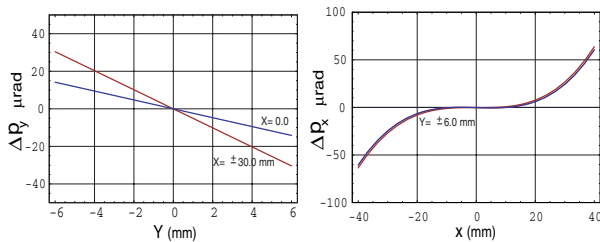


Figure 4: Transverse momentum kick produced by the one wiggler period.

vertical and horizontal kicks were computed by Eq.(4) for the particles whose coordinates do not exceed $X \pm 30$ mm and $Y \pm 6$ mm as shown in Fig. 4.

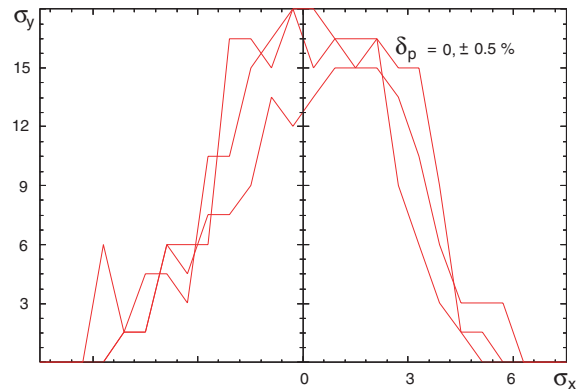


Figure 5: Dynamic aperture of the damping ring for the nonlinear wiggler field model.

REFERENCES

- [1] K. Halbach, FEB A95, LBL, 1995
- [2] M. Venturini, "Effect of wiggler insertions on the single-particle dynamics of the NLC main damping ring", LBNL-53264, July 2003.
- [3] E. Levitchev, P. Vobly, Workshop on wiggler optimization for emittance control, INFN-LNF, Frascati, 21-22 Feb, 2005.
- [4] J. Payet, BETA-LNS code